PHILOSOPHICAL MAGAZINE A, 2001, VOL. 81, NO. 4, 903–926

# Variational bounds for the effective moduli of heterogeneous piezoelectric solids

JIANG YU LI† and MARTIN L. DUNN‡

Center for Acoustics, Mechanics, and Materials, Department of Mechanical Engineering, University of Colorado, Boulder, Colorado 80309-0427, USA

[*Received 17 August 1998 and accepted in revised form 13 July 2000*]

ABSTRACT

Variational bounds for the effective moduli of heterogeneous piezoelectric solids are developed by generalizing the Hashin–Shtrikman variational principles. Narrower bounds than Voigt–Reuss-type bounds are obtained by taking into account both the inclusion shape and the volume fraction. The proposed bounds for the effective electroelastic moduli are applicable to statistically homogeneous multiphase composites of any microgeometry and anisotropy and are self-consistent. A prescription for the calculation of the bounds is presented that takes advantage of existing, often closed-form expressions for the piezoelectric Eshelby tensor for ellipsoidal inclusions. Numerical results are presented and compared with measurements for four composite materials with different microstructures. The Hashin–Shtrikman-type bounds are much narrower than the Voigt–Reuss-type bounds. In many but not all cases they are sufficiently narrow to serve as good estimates of various elastic, dielectric and piezoelectric moduli, as assessed by comparison with measurements. Furthermore, the average of the Voigt- and Reuss-type bounds (which is often used for elastic polycrystals and composites) does not in general accurately describe the effective moduli of the heterogeneous solid either quantitatively or qualitatively.

## §1. INTRODUCTION

Piezoelectric solids have at least two features that distinguish them from most elastic solids; electric and elastic fields in the solid are fully coupled, and they are inherently anisotropic. A further property of most piezoelectric materials is that of heterogeneity; heterogeneity that exists on multiple length scales. Piezoelectric crystals often contain complicated domain configurations, which are regions of different electrical polarizations. The permissible configurations are dictated by the symmetry of the crystal. This results in a variation in the elastic, piezoelectric and dielectric constants throughout the crystal; their values at a certain location depend on the orientation of the domain at that location. When a piezoelectric polycrystal is fabricated by standard ceramic processing techniques, the situation is even more complicated. Now, not only does each grain itself have a domain structure, but also the arrangement of the grains in the polycrystal leads to heterogeneity. Furthermore,

† Present address: Mail Code 104-44, California Institute of Technology, Pasadena, California 91125, USA.

‡ Author for correspondence. E-mail: dunnm@spot.colorado.edu

*Philosophical Magazine* A ISSN 0141–8610 print/ISSN 1460-6992 online 
http://www.tandf.co.uk/journals

upon processing, the elastic, electric and thermal anisotropy of the grains can lead to complicated internal electroelastic fields. These can include appreciable internal microstructural stresses. In order to relieve these stresses, domain reorientation and microcracking can occur and these in turn can substantially influence the overall response of the polycrystal. Furthermore, porosity often exists owing to sintering and this too affects the overall behaviour of the ceramic. On an even larger length scale, polycrystalline ceramic fibres are often embedded in a polymer matrix to form a piezoelectric composite. On this scale, it is really the effective properties of the ceramic fibres that influence the overall response of the composite. The distribution of the internal electroelastic fields in the composite microstructure of course determines the overall response. In this case, both internal electrical and mechanical fields couple.

The overall linear constitutive response of heterogeneous piezoelectric solids is of obvious technological importance. Recent efforts in this area can be categorized as obtaining either direct estimates of the effective moduli in terms of microstructural details (Newnham *et al*. 1978, Chan and Unsworth 1989, Grekov *et al*. 1989, Cao *et al*. 1992a,b, Dunn and Taya 1993a,b, Chen 1994, 1996), or exact connections between internal fields and various components of the effective moduli (Benveniste and Dvorak 1992, Chen 1993, Benveniste 1993a,b,c, 1994, Li and Dunn 1999). A third avenue of approach, which has only very recently been pursued, involves obtaining variational bounds on the effective moduli in terms of microstructural data. Such bounds not only provide estimates of the effective moduli (if they are sufficiently narrow) but also provide a rigorous means to validate micromechanics approximations. Since Hill (1952) first observed that Voigt (1889) and Reuss (1929) estimates provide bounds for effective elastic moduli, significant progress has been made in obtaining narrower bounds for uncoupled elastic moduli. Hashin and Shtrikman (1962, 1963) obtained bounds for an isotropic multiphase composite consisting of isotropic constituents using (what were then) new variational principles that they derived. Subsequently, Hill (1964) obtained bounds for the five effective moduli of a transversely isotropic fibre-reinforced composite with arbitrary transverse microgeometry. Walpole (1966,a,b, 1969) derived these bounds in a unified fashion, where the cases of disc-reinforced composites and anisotropic constituents were also included. Willis (1977, 1981) introduced the two-point correlation function into the Hashin–Shtrikman variational principle to represent a broader class of microstructures. When the two-point correlation function possesses radial, cylindrical or disc symmetry, the three results cited above are readily recovered. Weng (1992) explicitly evaluated the integral involved in the Willis bounds when the correlation function possesses ellipsoidal symmetry. He observed that, for matrix-based composites with aligned and identically shaped reinforcement, the effective moduli of the Mori–Tanaka (1973) mean-field approach correspond to the Willis upper (lower) bounds, when the matrix is the stiffest (most compliant) phase; otherwise it always lies between the Willis bounds. There are no variational bounds reported in the literature for multiphase composites with misaligned or differently shaped reinforcements, to the best knowledge of the present authors.

Despite the success of bounding approaches in uncoupled heterogeneous elasticity, only very recently have such approaches been applied to heterogeneous piezoelectric solids. Olson and Avellaneda (1992) obtained bounds for piezoelectric polycrystals with overall isotropic symmetry. As such, the overall solid is not piezoelectric. Bisegna and Luciano (1996) derived variational bounds for piezoelectric composites with periodic microgeometry. Hori and Nemat-Nasser (1998) have recently obtained universal bounds for effective piezoelectric moduli by generalizing the Hashin–Shtrikman variational principle and universal theorems that they established for uncoupled mechanical problems to piezoelectricity problems. To date, however, variational bounds have yet to be obtained explicitly for the effective electroelastic moduli of piezoelectric composites with general microgeometry. The present study intends to do just this. We first obtain a variational principle for heterogeneous piezoelectric solids with piecewise homogeneity. It is then used to bound the effective electroelastic moduli of matrix-based multiphase composites containing ellipsoidal reinforcement. The proposed bounds are applicable to statistically homogeneous multiphase composites of any microgeometry and anisotropy, with no statistical correlation function introduced. A procedure for calculation of the bounds for composites with ellipsoidal reinforcements is outlined that relies heavily on a new expression for the electroelastic Eshelby tensor for ellipsoidal inclusions, which takes advantage of existing expressions for the Eshelby tensor in the literature. Finally, numerical results are presented for four composite microgeometries and these are discussed in the context of measurements of the effective moduli.

## §2. Basic equations and notation

We consider linear electroelastic and, thus, inherently anisotropic media where electric and elastic fields are fully coupled. The field variables and material moduli are represented either by conventional indicial notation or by bold symbols. The constitutive equations for stationary linear response can be expressed as

$$\begin{aligned} \varepsilon_{ij} &= S_{ijkl}\sigma_{kl} + d_{ijk}E_k, \\ D_i &= d_{ikl}\sigma_{kl} + \tau_{ik}E_k, \end{aligned} \tag{1 a}$$

or

$$\begin{aligned} \sigma_{ij} &= C_{ijkl}\varepsilon_{kl} - h_{ijk}D_k, \\ E_i &= -h_{ikl}\varepsilon_{kl} + \beta_{ik}D_k. \end{aligned} \tag{1 b}$$

Here $\sigma_{ij}$ and $\varepsilon_{ij}$ are the elastic stress and strain respectively; $D_i$ and $E_i$ are the electric displacement and field respectively; $S_{ijkl}, d_{ijk}$ and $\tau_{ik}$ are the elastic compliance tensor (measured in a constant electric field), the piezoelectric tensor and the dielectric tensor (measured at a constant stress) respectively; $C_{ijkl}, h_{ijk}$ and $\beta_{ik}$ are the elastic stiffness tensor (measured in a constant electric displacement), the piezoelectric tensor and the dielectric tensor (measured at a constant strain) respectively. Note that different but equivalent constitutive equations can be written by making alternative choices of the dependent variables. We use this form because it leads to both a positive definite moduli matrix and a positive energy function.

To proceed, we adopt the shorthand notation of Barnett and Lothe (1975) that treats the elastic and electric variables on equal footing. It is similar to conventional indicial notation with the exception that both lower-case and upper-case subscripts are used as indices. Lower-case subscripts take the range 1–3, while upper-case subscripts take the range 1–4, and repeated upper-case subscripts are summed over $1 \rightarrow 4$. With this notation, the field quantities are expressed as:

$$X_{iJ} = \begin{cases} \varepsilon_{ij}, & J = 1,2,3, \\ D_i, & J = 4, \end{cases} \qquad Y_{Ji} = \begin{cases} \sigma_{ji}, & J = 1,2,3, \\ E_i, & J = 4. \end{cases} \tag{2}$$

The electroelastic moduli are expressed as

$$P_{iJKl} = \begin{cases} S_{ijkl}, & J, K = 1, 2, 3, \\ d_{ijl}, & J = 1, 2, 3, K = 4, \\ d_{ikl}, & J = 4, K = 1, 2, 3, \\ \tau_{il}, & J, K = 4, \end{cases} \tag{3}$$

The inverse of $P_{iJKl}$ is denoted as $Q_{AbiJ}$. It contains the tensors $C_{ijkl}$, $-h_{ijk}$ and $\beta_{ik}$. With this shorthand notation, we can rewrite equations (1) as

$$X_{iJ} = P_{iJKl} Y_{Kl}, \qquad Y_{Kl} = Q_{KliJ} X_{iJ}. \tag{4}$$

Note that both $P_{iJKl}$ and $Q_{KliJ}$ are positive definite.

For the heterogeneous materials considered here, we define the effective electroelastic constitutive equation in a statistical sense, under the assumption of macroscopic homogeneity:

$$\langle X_{iJ} \rangle = P^*_{iJKl} \langle Y_{Kl} \rangle, \qquad \langle Y_{Kl} \rangle = Q^*_{KliJ} \langle X_{iJ} \rangle. \tag{5}$$

Here $\langle\,\rangle = (1/V) \int_V (\,)\, dV$ denotes the average of a quantity, over the volume of the heterogeneous solid. In equations (5), $P^*_{iJKl}$ and $Q^*_{KliJ}$ are the effective electroelastic moduli. It is understood that, in general, all the properties of the heterogeneous solid, except for the effective properties, are functions of the position $\mathbf{x}$; however, to simplify notation such a dependence is indicated only when necessary.

## §3. Variational principles: bounds for effective electroelastic moduli

### 3.1. *Minimum energy theorem*

Let $V$ denote the volume of a heterogeneous solid bounded by a surface denoted by $S$. Consider the mixed uniform boundary conditions defined by

$$u_i = u_i^0, \qquad \mathbf{x} \in S_{m1}, \qquad \sigma_{ij} = \sigma_{ij}^0, \qquad \mathbf{x} \in S_{m2}, \tag{6a}$$

$$D_i = D_i^0, \qquad \mathbf{x} \in S_{e1}, \qquad \phi = \phi^0, \qquad \mathbf{x} \in S_{e2}, \tag{6b}$$

where $u_i$ and $\phi$ are the elastic displacement and electric potential respectively, and $S_{m1}, S_{m2}, S_{e1}$ and $S_{e2}$ are subregions of $S$ that satisfy the following requirements:

$$S_{m1} \cup S_{m2} = S, \qquad S_{m1} \cap S_{m2} = \varnothing, \qquad S_{e1} \cup S_{e2} = S, \qquad S_{e1} \cap S_{e2} = \varnothing.$$

Let us define two potentials $\Phi$ and $\Psi$ as

$$\Phi(\tilde{Y}_{Ji}) = \tfrac{1}{2} \int_V \tilde{Y}_{Ji} P_{iJKl} \tilde{Y}_{Kl}\, dV - \int_{S_{m1}} (\tilde{\sigma}_{ij} n_j) u_i^0\, dS + \int_{S_{e1}} (D_i^0 n_i) \tilde{\phi}\, dS, \tag{7a}$$

$$\Psi(\tilde{X}_{iJ}) = \tfrac{1}{2} \int_V \tilde{X}_{iJ} Q_{JikL} \tilde{X}_{kL}\, dV - \int_{S_{m2}} (\sigma_{ij}^0 n_j) \tilde{u}_i\, dS + \int_{S_{e2}} (\tilde{D}_i n_i) \phi^0\, dS, \tag{7b}$$

where $n_i$ is the normal to the surface. For $\Phi(\tilde{Y}_{Ji})$ in equation (7 *a*), $\tilde{Y}_{kl}$ is a trial field that satisfies the specified boundary conditions, equilibrium equations and gradient equations on $Y_{Kl}(\mathbf{x})$, but the resulting $\tilde{X}_{iJ} = P_{iJKl} \tilde{Y}_{Kl}$ may not satisfy the boundary conditions, equilibrium equations and gradient equations on $X_{iJ}(\mathbf{x})$. On the other hand, for $\Psi(\tilde{X}_{iJ})$ in equation (7 *b*), $\tilde{X}_{iJ}$ is a trial field that satisfies the boundary conditions, equilibrium equations and gradient equations on $X_{iJ}(\mathbf{x})$, but the resulting $\tilde{Y}_{Kl} = Q_{KliJ} \tilde{X}_{iJ}$ may not satisfy the specified boundary conditions, equilibrium equations and gradient equations on $Y_{Kl}(\mathbf{x})$. We can prove two minimum potential theorems that state that the actual fields $Y_{Ji}(\mathbf{x})$ and $X_{iJ}(\mathbf{x})$ in the heterogeneous solid minimize the potentials $\Phi$ and $\Psi$ respectively. To this end, we define $\tilde{Y}_{Ji} = Y_{Ji} + Y'_{Ji}$, substitute it into equation (7 *a*) and perform the following calculation:

$$
\begin{aligned}
\Phi(\tilde{Y}_{Ji}) - \Phi(Y_{Ji}) &= \tfrac{1}{2}\int_V Y'_{Ji}P_{iJKl}Y'_{Kl}\,dV + \int_V Y'_{Ji}P_{iJKl}Y_{Kl}\,dV - \int_{S_{m1}} (\sigma'_{ij}n_j)u_i^0\,dS \\
&\quad + \int_{S_{e1}} (D_i^0 n_i)\phi'\,dS \\
&= \tfrac{1}{2}\int_V Y'_{Ji}P_{iJKl}Y'_{Kl}\,dV + \int_V \sigma'_{ij}\varepsilon_{ij}\,dV + \int_V E'_i D_i\,dV \\
&\quad - \int_{S_{m1}} (\sigma'_{ij}n_j)u_i^0\,dS + \int_{S_{e1}} (D_i^0 n_i)\phi'\,dS \\
&= \tfrac{1}{2}\int_V Y'_{Ji}P_{iJKl}Y'_{Kl}\,dV + \int_S \sigma'_{ij}u_i n_j\,dS - \int_S \phi' D_i n_i\,dS \\
&\quad - \int_{S_{m1}} (\sigma'_{ij}n_j)u_i^0\,dS + \int_{S_{e1}} (D_i^0 n_i)\phi'\,dS \\
&= \tfrac{1}{2}\int_V Y'_{Ji}P_{iJKl}Y'_{Kl}\,dV + \int_{S_{m2}} (\sigma'_{ij}n_j)u_i\,dS - \int_{S_{e2}} \phi' D_i n_i\,dS \\
&= \tfrac{1}{2}\int_V Y'_{Ji}P_{iJKl}Y'_{Kl}\,dV \\
&\geqslant 0.
\end{aligned}
$$

The last inequality comes from the positive definiteness of $P_{iJKl}$. This proves that the actual field $Y_{Ji}(\mathbf{x})$ minimizes the potential $\Phi$. A similar calculation can be performed to prove that $X_{iJ}(\mathbf{x})$ minimizes the potential $\Psi$. Note that, in the derivation, the elastic and electrostatic equilibrium equations have been used.

Now let us consider applied traction and electric potential boundary conditions on the surface *S* of the heterogeneous solid, consistent with a uniform stress and electric field $Y^0_{Ji}$, that is

$$Y_{Ji}(\mathbf{x}) = Y^0_{Ji}, \quad \mathbf{x} \in S.$$

Making use of relevant averaging theorems for heterogeneous electroelastic solids (Dunn and Taya 1993a), we have $\langle Y_{Ji}\rangle = Y^0_{Ji}$. The resulting internal energy density in the heterogeneous solid is

$$U = \tfrac{1}{2}\langle Y_{Ji}P_{iJKl}Y_{Kl}\rangle = \tfrac{1}{2}\langle Y_{Ji}\rangle P^*_{iJKl}\langle Y_{Kl}\rangle. \tag{8}$$

These boundary conditions correspond to

$$S_{m2} = S, \quad S_{m1} = \varnothing, \quad S_{e2} = S, \quad S_{e1} = \varnothing,$$

so that $U = \tfrac{1}{2}\langle Y_{Ji}P_{iJKl}Y_{Kl}\rangle = \Phi_{min}/V$. According to the minimum-potential theorem, the internal energy density is minimized by the actual field $Y_{Ji}(\mathbf{x})$:

$$2U \leqslant \langle \tilde{Y}_{Ji}P_{iJKl}\tilde{Y}_{Kl}\rangle. \tag{9}$$

Substituting equation (8) into equation (9) yields

$$(\langle Y_{Ji}\rangle P^{*}_{iJKl}\langle Y_{Kl}\rangle) \leqslant (\langle \tilde{Y}_{Ji} P_{iJKl} \tilde{Y}_{Kl}\rangle). \tag{10 a}$$

A similar result can be obtained for applied elastic and electric displacement boundary conditions:

$$(\langle X_{iJ}\rangle Q^{*}_{JikL}\langle X_{kL}\rangle) \leqslant (\langle \tilde{X}_{iJ} Q_{JikL} \tilde{X}_{kL}\rangle). \tag{11 a}$$

By Legendre transformation, we can also derive

$$(\langle Y_{Ji}\rangle P^{*}_{iJKl}\langle Y_{Kl}\rangle) \geqslant (\langle \tilde{X}_{iJ} (2Y^{0}_{Ji} - Q_{JikL} \tilde{X}_{kL})\rangle) \tag{10 b}$$

and

$$(\langle X_{iJ}\rangle Q^{*}_{JikL}\langle X_{kL}\rangle) \geqslant (\langle \tilde{Y}_{Ji} (2X^{0}_{iJ} - P_{iJMn} \tilde{Y}_{Mn})\rangle). \tag{11 b}$$

Equations (10) and (11) show that, by choosing appropriate trial fields, we can give the bounds for the effective electroelastic moduli $P^{*}_{iJKl}$ and $Q^{*}_{JikL}$.

### 3.2. *Voigt–Reuss-type bounds*

From now on we shall consider the traction–electric potential boundary conditions and elastic displacement–electric displacement boundary conditions in a parallel manner. The simplest trial field is the uniform field compatible with the boundary conditions:

$$\tilde{Y}_{Kl} = Y^{0}_{Kl} \quad \text{or} \quad \tilde{X}_{iJ} = X^{0}_{iJ}. \tag{12}$$

Substituting equations (12) into equations (10) and (11) yields

$$P^{*}_{iJKl} \leqslant \langle P_{iJKl}\rangle \quad \text{or} \quad Q^{*}_{JikL} \leqslant \langle Q_{JikL}\rangle. \tag{13}$$

Recall that both $P_{iJKl}$ and $Q_{JikL}$ are positive definite. Also note that the inequality in equation (13) is used to indicate the positive or negative definiteness between matrices. Equations (13) provide upper bounds for the effective electroelastic moduli $P^{*}_{iJKl}$ and $Q^{*}_{JikL}$ of a heterogeneous electroelastic solid. Inverting equations (13) then yields

$$Q^{*}_{JikL} \geqslant \langle Q^{-1}_{JikL}\rangle^{-1}, \quad P^{*}_{iJKl} \geqslant \langle P^{-1}_{iJKl}\rangle^{-1}. \tag{14}$$

Equations (14) provide lower bounds for the effective electroelastic moduli $Q^{*}_{JikL}$ and $P^{*}_{iJKl}$ of a heterogeneous electroelastic solid. It is clear that the upper bounds of $P^{*}_{iJKl}$ and $Q^{*}_{JikL}$ correspond to the inverses of the lower bounds of $Q^{*}_{JikL}$ and $P^{*}_{iJKl}$. Equations (13) and (14) correspond to the classical Voigt (1889) and Reuss (1929) bounds in heterogeneous elastic solids.

### 3.3. *Hashin–Shtrikman-type bounds*

The Voigt–Reuss bounds are known to provide an accurate estimate of the effective elastic moduli of heterogeneous solids when the elastic mismatch between the different phases in a multiphase composite is small, or when the elastic anisotropy in a polycrystalline material is weak. In the case of large property mismatch or strong anisotropy, as is usually the case with piezoelectric composites, the Voigt–Reuss bounds are too wide for practical applications (we shall show and discuss this later). The objective of this section is to obtain narrower bounds for the effective electroelastic moduli of heterogeneous piezoelectric solids. The work is motivated by the original work of Hashin and Shtrikman (1962, 1963) and Walpole (1966a,b,

1969) in uncoupled heterogeneous elasticity. Hashin and Shtrikman derived a variational principle and used it to bound the effective elastic moduli of spherical-particle-reinforced composites. Walpole used a different but equivalent formalism to obtain bounds for composites reinforced by spherical particles, cylindrical fibres and thin discs in a unified fashion. Willis (1977) introduced the two-point correlation function into the Hashin–Shtrikman variational principle to represent a broader class of microgeometries. Weng (1992) evaluated the Willis bounds explicitly for the case when the reinforcement was ellipsoidal. It is clear from the Walpole formalism that the evaluation of the Hashin–Shtrikman-type bounds depends on the availability of the solution to the auxiliary problem of a single inclusion in an infinite solid. Such a realization allows the extension from isotropic to anisotropic solids, and from spherical to ellipsoidal inclusion shapes. For this reason we follow the Walpole approach, generalize the uncoupled elastic Hashin–Shtrikman principle to coupled piezoelectric solids and use it to bound the effective electroelastic moduli of heterogeneous piezoelectric solids with ellipsoidal reinforcement. As we shall show later, the variational bounds that we developed are applicable to statistically homogeneous multiphase composites with any microgeometry and anisotropy, such as composites with misaligned or differently shaped reinforcements, and do not require a particular statistical correlation function.

It is well known that the introduction of a convenient comparison material together with an arbitrarily assignable eigenfield facilitates the analysis of the boundary-value problems for heterogeneous media. To this end let us introduce a comparison material of homogeneous electroelastic moduli $P^0_{iJKl}$ and $Q^0_{JikL}$ with an arbitrarily assignable eigenfield $Y^T_{Kl}(\mathbf{x})$ and $X^T_{iJ}(\mathbf{x})$, subjected to the same boundary conditions as the heterogeneous material, that is $\langle \tilde{Y}_{Kl} \rangle = Y^0_{Kl}$ or $\langle \tilde{X}_{iJ} \rangle = X^0_{iJ}$. Note that now $\tilde{Y}_{Kl}$ and $\tilde{X}_{iJ}$ denote the actual electroelastic fields in the comparison material. They will also be used as the trial fields in equations (10) and (11) to bound the effective moduli $P^*_{iJKl}$ and $Q^*_{JikL}$ since they satisfy all the requirements of trial fields. The electroelastic fields in the comparison material are then connected by the constitutive equations

$$\tilde{X}_{iJ} = P^0_{iJKl}(\tilde{Y}_{Kl} - Y^T_{Kl}), \quad \tilde{Y}_{Ji} = Q^0_{JiKl}(\tilde{X}_{Kl} - X^T_{Kl}). \tag{15}$$

The eigenfield $Y^T_{Kl}$ is introduced to make $\tilde{\varepsilon}_{ij} = \tilde{u}_{i,j}$ and $\tilde{D}_{i,i} = 0$, and $X^T_{iJ}$ is introduced to make $\tilde{\sigma}_{ij,i} = 0$ and $\tilde{E}_i = -\tilde{\varphi}_i$, so that $\tilde{Y}_{Kl}$ and $\tilde{X}_{iJ}$ satisfy the equilibrium and gradient equations. Their influence may be imagined to be due to a certain distribution of body force and electric charge, as is well known from Eshelby's (1957, 1959) work on elastic inclusions. The choice of $Y^T_{Kl}$ and $X^T_{iJ}$ will generate $\tilde{X}_{iJ}$ and $\tilde{Y}_{Kl}$, which are approximations to the actual fields in the considered region of the heterogeneous solid.

At this point, no assumptions have been made regarding the specific microstructure of the heterogeneous solid, and the derivation is general. To apply the analysis, we focus on piecewise uniform heterogeneous materials with *n* distinct phases. Such materials can be described by electroelastic moduli of the form

$$P_{iJKl} = \sum_r \Theta_r(\mathbf{x}) P_{iJKL}|_r, \quad Q_{JikL} = \sum_r \Theta_r(\mathbf{x}) Q_{JikL}|_r, \tag{16}$$

where $|_r$ denotes a quantity of phase *r*, and $\Theta_r(\mathbf{x})$ is a characteristic function that describes the topology of the microstructure, that is

$$\Theta_r(\mathbf{x}) = \begin{cases} 1, & \mathbf{x} \in r, \\ 0, & \mathbf{x} \notin r. \end{cases} \tag{17}$$

Note that both multiphase composites and polycrystals can be represented by this notation. An important property of $\Theta_r(\mathbf{x})$ is that $\langle G(\mathbf{x})\Theta_r(\mathbf{x})\rangle = c_r\langle G(\mathbf{x})|_r\rangle$ where $G(\mathbf{x})$ is any material property that varies throughout the microstructure and $c_r$ is the volume fraction of phase *r*.

To bound the electroelastic moduli $P^*_{iJKl}$ and $Q^*_{JikL}$, the crucial step is to choose appropriate trial fields $\tilde{Y}_{Kl}$ and $\tilde{X}_{iJ}$, which in turn imply $Y^T_{Kl}$ and $X^T_{iJ}$. For piecewise uniform heterogeneous materials, a piecewise uniform eigenfield is the most general that permits calculation of the required average values solely in terms of the given information. To this end we choose

$$Y^T_{Kl}(\mathbf{x}) = \sum_r \Theta_r(\mathbf{x})Y^T_{Kl}|_r, \quad X^T_{iJ}(\mathbf{x}) = \sum_r \Theta_r(\mathbf{x})X^T_{iJ}|_r, \tag{18}$$

with

$$Y^T_{Kl}|_r = Q^0_{KliJ}(P^0_{iJAb} - P_{iJAb}|_r)\bar{Y}_{Ab}|_r, \quad X^T_{iJ}|_r = P^0_{iJKl}(Q^0_{KlbA} - Q_{KlbA}|_r)\bar{X}_{bA}|_r. \tag{19}$$

Here $\bar{Y}_{Ab}|_r = \langle\tilde{Y}_{Ab}|_r\rangle$ and $\bar{X}_{bA}|_r = \langle\tilde{X}_{bA}|_r\rangle$ are the volume averages of $\tilde{Y}_{Ab}$ and $\tilde{X}_{bA}$ over phase *r* in the homogeneous comparison materials. Equation (15) can then be rewritten as

$$\tilde{X}_{iJ}|_r = P_{iJKl}|_r\bar{Y}_{Kl}|_r + P^0_{iJKl}Y'_{Kl}|_r, \quad \tilde{Y}_{Kl}|_r = Q_{KliJ}|_r\bar{X}_{iJ}|_r + Q^0_{KliJ}X'_{iJ}|_r, \tag{20}$$

with

$$Y'_{Kl}|_r = \tilde{Y}_{Kl}|_r - \bar{Y}_{Kl}|_r, \quad X'_{iJ}|_r = \tilde{X}_{iJ}|_r - \bar{X}_{iJ}|_r. \tag{21}$$

The generalized Hill condition (for example Kreher and Pompe (1989) and Li and Dunn (1999)) for heterogeneous piezoelectric solids subjected to uniform boundary conditions can be written as

$$\langle X_{iJ}Y_{Ji}\rangle = \langle X_{iJ}\rangle\langle Y_{Ji}\rangle. \tag{22}$$

The generalized Hill condition is valid for

(i) statistical homogeneous materials,
(ii) where no body force or free charge exists so that equilibrium is satisfied and
(iii) where the strain and electric field are derivable from the elastic displacement and electric potential.

$X_{iJ}$ and $Y_{Ji}$ need not be connected by any certain constitutive equation. Applying the generalized Hill condition to $\tilde{Y}_{Ji}$ and $\tilde{X}_{iJ}$ yields

$$\langle\tilde{X}_{iJ}(Y^0_{Ji} - \tilde{Y}_{Ji})\rangle = 0, \quad \langle\tilde{Y}_{Ji}(X^0_{iJ} - \tilde{X}_{iJ})\rangle = 0. \tag{23}$$

Adding the left-hand sides of equations (23) to the right-hand sides of equations (10) and (11) respectively, followed by the substitution of $\tilde{Y}_{Ji}|_r$ and $\tilde{X}_{iJ}|_r$ from equations (20), the inequalities of the minimum-energy theorems can be written as

$$2U \leqslant \sum_r c_r Y^0_{Ji}P_{iJKl}|_r\bar{Y}_{Kl}|_r - \langle Y'_{Ji}|_r(P^0_{iJKl} - P_{iJKl}|_r)Y'_{Kl}|_r\rangle, \tag{24 a}$$

$$2U \leqslant \sum_r c_r X^0_{iJ}Q_{JikL}|_r\bar{X}_{kL}|_r - \langle X'_{iJ}|_r(Q^0_{JikL} - Q_{JikL}|_r)X'_{kL}|_r\rangle. \tag{24 b}$$

Equations (24) are the piezoelectric analogue of the Hashin–Shtrikman (1962, 1963) variational principle. In order to bound the effective electroelastic moduli of heterogeneous piezoelectric solids using equations (24), we introduce the concentration factors $\bar{A}_{AbMn}|_r$ and $\bar{B}_{iJkL}|_r$ that are defined by $\bar{Y}_{Ab}|_r = \bar{A}_{AbMn}|_r Y^0_{Mn}$ and $\bar{X}_{iJ}|_r = \bar{B}_{iJkL}|_r X^0_{kL}$. Equations (24) can then be rewritten as

$$2U \leqslant \sum_r c_r Y^0_{Ji} P_{iJKl}|_r \bar{A}_{KlAb}|_r Y^0_{Ab} - \langle Y'_{Ji}|_r (P^0_{iJKl} - P_{iJKl}|_r) Y'_{Kl}|_r \rangle, \tag{25 a}$$

$$2U \leqslant \sum_r c_r X^0_{iJ} Q_{JikL}|_r \bar{B}_{kLmN}|_r X^0_{mN} - \langle X'_{iJ}|_r (Q^0_{JikL} - Q_{JikL}|_r) X'_{kL}|_r \rangle. \tag{25 b}$$

These can be written as

$$Y^0_{Ji}(P^*_{iJKl} - \bar{P}_{iJKl}) Y^0_{Kl} \leqslant -\sum_r \langle Y'_{Ji}|_r (P^0_{iJKl} - P_{iJKl}|_r) Y'_{Kl}|_r \rangle, \tag{26 a}$$

$$X^0_{iJ}(Q^*_{JikL} - \bar{Q}_{JikL}) X^0_{kL} \leqslant -\sum_r \langle X'_{Ji}|_r (Q^0_{JikL} - Q_{JikL}|_r) X'_{kL}|_r \rangle, \tag{26 b}$$

with the definitions

$$\bar{P}_{iJAb} = \sum_r c_r P_{iJKl}|_r \bar{A}_{KlAb}|_r, \quad \bar{Q}_{JimN} = \sum_r c_r Q_{JikL}|_r \bar{B}_{kLmN}|_r. \tag{27}$$

A similar derivation following from equations (10 *b*) and (11 *b*) gives us

$$Y^0_{Ji}(P^*_{iJKl} - \bar{P}_{iJKl}) Y^0_{Kl} \geqslant \sum_r \langle Y'_{Ji}|_r P^0_{iJKl}(Q^0_{KlmN} - Q_{KlmN}|_r) P^0_{mNOp} Y'_{Op}|_r \rangle, \tag{26 c}$$

$$X^0_{iJ}(Q^*_{JikL} - \bar{Q}_{JikL}) X^0_{kL} \geqslant \sum_r \langle X'_{iJ}|_r Q^0_{JikL}(P^0_{kLMn} - P_{kLMn}|_r) Q^0_{MnoP} X'_{oP}|_r \rangle. \tag{26 d}$$

Hence from equations (26) it follows that the effective electroelastic moduli are bounded by the two following theorems.

(*a*) If $P^0_{iJKl} - P_{iJKl}|_r$ is positive (negative) semidefinite, so is $\bar{P}_{iJKl} - P^*_{iJKl}$.

(*b*) If $Q^0_{JikL} - Q_{JikL}|_r$ is positive (negative) semidefinite, so is $\bar{Q}_{JikL} - Q^*_{JikL}$.

By choosing comparison materials more positive or negative definite than the constituent materials, we can obtain upper or lower bounds for $P^*_{iJKl}$ and $Q^*_{JikL}$ represented by $\bar{P}_{iJKl}$ and $Q_{JikL}$. Hashin and Shtrikman (1962, 1963) first obtained such bounds for heterogeneous elastic solids. It is noted that it is the exact average fields $\bar{Y}_{Ab}|_r$ and $\bar{X}_{iJ}|_r$ in the inclusion, rather than the exact field distribution $\tilde{Y}_{Ab}|_r(\mathbf{x})$ and $\tilde{X}_{iJ}|_r(\mathbf{x})$, that determine the variational bounds on the effective electroelastic moduli. This observation enables us to determine the bounds rigorously for multi-phase composites with a wide range of microgeometries, as we show later.

### 3.4. *Computation of the approximate electroelastic fields*

The only assumptions made in the derivation so far are those of statistical and piecewise homogeneity. Otherwise we have retained complete generality concerning the details of the heterogeneous microstructure. Now we apply the general theory to a matrix-based composite consisting of *n* phases, where phase 1 denotes the matrix and phases 2 to *n* are inhomogeneities, not necessarily ellipsoidal. It is understood that inhomogeneities of different shapes or different alignments relative to a sample coordinate system are considered different phases. Note that the general results can also be applied to a piezoelectric polycrystal where we regard grains of different orientations as different phases; however, we shall not pursue that line of inquiry. To obtain the upper and lower bounds on the effective electroelastic moduli, we need

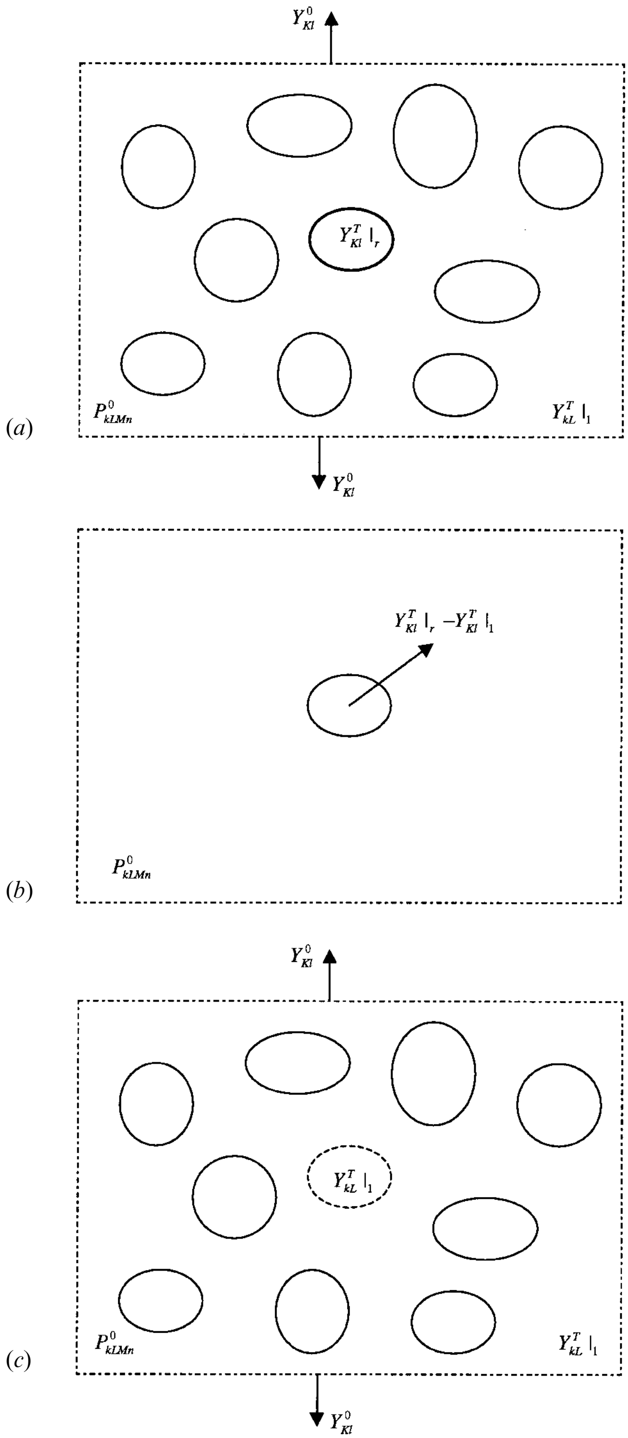


Figure 1. Piezoelectric inclusion problem: (*a*) original problem with eigenfield $Y^{\mathrm{T}}_{Kl}|_r$ in inclusion and $Y^{\mathrm{T}}_{Kl}|_1$ in matrix; (*b*) a single inclusion problem with eigenfield $Y^{\mathrm{T}}_{Kl}|_r - Y^{\mathrm{T}}_{Kl}|_1$; (*c*) identical with (*a*), with the exception that in one inclusion the eigenfield is changed to $Y^{\mathrm{T}}_{Kl}|_1$, the same as that in the matrix.

to determine $\bar{A}_{AbMn}|_r$ and $\bar{B}_{iJkL}|_r$ in equations (27). It is clear from the definition of $\bar{A}_{AbMn}|_r$ and $\bar{B}_{iJkL}|_r$ that this is an inclusion problem, where we need to solve for the average electroelastic fields inside the inclusion that are caused by both the eigenfields $Y^T_{Kl}$ or $X^T_{iJ}$ in the inclusion and the applied external loading $Y^0_{Kl}$ or $X^0_{iJ}$ at the boundary. The problem is demonstrated in figure 1. We are considering a matrix of electrostatic moduli $P^0_{kLMn}$ and eigenfield $Y^T_{Kl}|_1$, and $n-1$ different phases of inclusions, which have the identical electrostatic moduli with the matrix, but different eigenfields $Y^T_{Kl}|_r (r = 2 \rightarrow n)$ (see figure 1 (*a*)). The shapes and alignments of the inclusions may also be different. We are interested in the average field in the inclusion highlighted in figure 1 (*a*). By statistical homogeneity, this average field is also equal to the average field in phase *r*. Owing to the linearity, the problem can be decomposed into two problems: one is a single inclusion with eigenfield $Y^T_{Kl}|_r - Y^T_{Kl}|_1$ embedded in the matrix without an eigenfield and subjected to no external loading (see figure 1 (*b*)); the other is identical with the original problem, with the exception that the eigenfield in the considered inclusion highlighted in figure 1 (*a*) is changed to $Y^T_{Kl}|_1$ (see figure 1 (*c*)). So the average field in the considered inclusion can be expressed as

$$\bar{Y}_{Ji}|_r = \bar{Y}_{Ji}|_{1r} + \bar{Y}_{Ji}|_{2r}, \quad \bar{X}_{iJ}|_r = \bar{X}_{iJ}|_{1r} + \bar{X}_{iJ}|_{2r}, \tag{28 a}$$

where the subscripts $1r$ and $2r$ are used to denote the average field in the considered inclusion shown in figure 1 (*b*) and (*c*) respectively. Let us first consider $Y_{Ji}|_{1r}$, the average field in a single inclusion shown in figure 2 (*b*). Owing to linearity, we have

$$\bar{Y}_{Ji}|_{1r} = S^Y_{JiKl}|_r (Y^T_{Kl}|_r - Y^T_{Kl}|_1), \quad \bar{X}_{iJ}|_{1r} = S^X_{iJkL}|_r (X^T_{kL}|_r - X^T_{kL}|_1), \tag{28 b}$$

where $S^Y_{JiKl}|_r$ and $S^X_{iJkL}|_r$ are functions of electroelastic moduli of matrix, and the inclusion shape. It is noted that equation (28 *b*) can be applied not only to ellipsoidal inclusion but also to any inclusion with arbitrary shape, as long as its average field can be evaluated. The matrix, however, still needs to be infinite, to keep the translational invariance assured by the property of the infinite-body Green's function. The fact that a uniform field exists in an ellipsoidal inclusion embedded in an infinite matrix provides a convenient way to evaluate the average field, but this feature is not essential from a theoretical point of view. Only in the case of ellipsoidal inclusion embedded in an infinite matrix do $S^Y_{JiKl}|_r$ and $S^X_{iJkL}|_r$ correspond to the piezoelectric Eshelby tensor. In all other cases, they are tensors connecting the eigenfield in the inclusion and the resulting average field; its validity is assured by the linear piezoelectricity. For the inclusion in figure 2 (*c*), it should be noted that it is actually not an inclusion problem, since it has the same electroelastic moduli $P^0_{kLMn}$ and eigenfield $Y^T_{Kl}|_1$ as the matrix. In fact, it is just a part of the matrix. From the assumption of statistical homogeneity, its average field should be equal to the average field of the matrix, which is denoted as $Y^I_{Ji}$. Since the only difference between figures 1 (*a*) and (*c*) is the eigenfield in a single inclusion, the average field in matrix in these two situations should be identical (a single inclusion will not change the average field in the matrix, since its volume fraction is zero). Thus, the solution of the electroelastic inclusion problem shown in figure 1 (*a*) can be expressed as

$$\bar{Y}_{Ji}|_r = S^Y_{JiKl}|_r (Y^T_{Kl}|_r - Y^T_{Kl}|_1) + Y^I_{Ji}, \quad \bar{X}_{iJ}|_r = S^X_{iJkL}|_r (X^T_{kL}|_r - X^T_{kL}|_1) + X^I_{iJ} \tag{28 c}$$

for phases $2 - n$, and

$$\bar{Y}_{Ji}|_1 = Y^I_{Ji}, \quad \bar{X}_{iJ}|_1 = X^I_{iJ} \tag{28 d}$$

for the matrix. Equations (28 *c*) and (28 *d*) are the exact solution for inclusion with arbitrary shape embedded in an infinite matrix, as long as the resulting composite is statistically homogeneous. Note that $S^{Y}_{JiKl}|_r$ and $S^{X}_{iJkL}|_r$ are functions of the electroelastic moduli $P^0_{iJMn}$ of comparison material and the shape of the constituent phase *r*. They are related to the Eshelby tensor $S_{JiKl}$ for piezoelectric solids defined by Dunn and Taya (1993a) in the case of an ellipsoidal inclusion. Complete details regarding this connection and its use are given in Appendix A. $S^{Y}_{JiKl}|_r(Y^{T}_{Kl}|_r - Y^{T}_{Kl}|_1)$ and $S^{X}_{iJkL}|_r(X^{T}_{kL}|_r - X^{T}_{kL}|_1)$ are the electroelastic fields in the inclusion caused by the eigenfields $Y^{T}_{Kl}$ and $X^{T}_{kL}$, and $Y^{I}_{Kl}$ and $X^{I}_{kL}$ are image fields that account for the applied external loading and interactions among inclusions. Substituting equations (19) into equation (28 *c*) yields

$$\bar{Y}_{Ji}|_r = S^{Y}_{JiKl}|_r[Q^0_{KlmN}(P^0_{mNAb} - P_{mNAb}|_r)\bar{Y}_{Ab}|_r - Q^0_{KlmN}(P^0_{mNAb} - P_{mNAb}|_1)Y^{I}_{Ab}] + Y^{I}_{Ji}, \tag{29 a}$$

$$\bar{X}_{iJ}|_r = S^{X}_{iJkL}|_r[P^0_{kLAb}(Q^0_{AbmN} - Q_{AbmN}|_r)\bar{X}_{mN}|_r - P^0_{kLAb}(Q^0_{AbmN} - Q_{AbmN}|_1)X^{I}_{mN}] + X^{I}_{iJ}. \tag{29 b}$$

Rearranging the terms in equations (29) yields

$$\bar{Y}_{Ab}|_r = A_{AbJi}|_r A^{-1}_{JiKl}|_{1r} Y^{I}_{Kl}, \quad \bar{X}_{bA}|_r = B_{bAiJ}|_r B^{-1}_{iJkL}|_{1r} X^{I}_{kL}, \quad r = 2 - n, \tag{30}$$

where

$$A_{JiAb}|_r = [I_{JiAb} + S^{Y}_{JiKl}|_r Q^0_{KlmN}(P_{mNAb}|_r - P^0_{mNAb})]^{-1}, \quad r = 2 - n, \tag{31 a}$$

$$B_{iJmN}|_r = [I_{iJmN} + S^{X}_{iJkL}|_r P^0_{kLAb}(Q_{AbmN}|_r - Q^0_{AbmN})]^{-1}, \quad r = 2 - n, \tag{31 b}$$

$$A_{JiAb}|_{1r} = [I_{JiAb} + S^{Y}_{JiKl}|_r Q^0_{KlmN}(P_{mNAb}|_1 - P^0_{mNAb})]^{-1}, \quad r = 2 - n, \tag{31 c}$$

$$B_{iJmN}|_{1r} = [I_{iJmN} + S^{X}_{iJkL}|_r P^0_{kLAb}(Q_{AbmN}|_1 - Q^0_{AbmN})]^{-1}, \quad r = 2 - n, \tag{31 d}$$

where $I_{JiAb}$ is a group of second- and fourth-rank unitary tensors. Since $\Sigma_r c_r \bar{Y}_{Ji}|_r = Y^0_{Ji}$ and $\Sigma_r c_r \bar{X}_{iJ}|_r = X^0_{iJ}$, we have

$$Y^{I}_{Ji} = \left(\sum_{r=2}^{n} c_r A_{JiMn}|_r A^{-1}_{MnAb}|_{1r} + c_1 I_{JiAb}\right)^{-1} Y^0_{Ab}, \tag{32 a}$$

$$X^{I}_{iJ} = \left(\sum_{r=2}^{n} c_r B_{iJmN}|_r B^{-1}_{mNaB}|_{1r} + c_1 I_{iJaB}\right)^{-1} X^0_{aB}. \tag{32 b}$$

Substituting equations (32) into equations (30) yields

$$\bar{Y}_{Kl}|_r = A_{KlCd}|_r \left[\left(\sum_{r=2}^{n} c_r A_{JiMn}|_r A^{-1}_{MnAb}|_{1r}\right) A_{CdJi}|_{1r} + c_1 A_{CdAb}|_{1r}\right]^{-1} Y^0_{Ab}, \tag{33 a}$$

$$\bar{X}_{kL}|_r = B_{kLcD}|_r \left[\left(\sum_{r=2}^{n} c_r B_{iJmN}|_r B^{-1}_{mNaB}|_{1r}\right) B_{cDiJ}|_{1r} + c_1 B_{cDaB}|_{1r}\right]^{-1} X^0_{aB}, \tag{33 b}$$

which then leads to:

$$\bar{A}_{KlAb}|_r = A_{KlCd}|_r \left[ \left( \sum_{r=2}^{n} c_r A_{JiMn}|_r A^{-1}_{MnAb}|_{1r} \right) A_{CdJ}|_{1r} + c_1 A_{CdAb}|_{1r} \right]^{-1},$$

$$r = 2 - n, \tag{34 a}$$

$$\bar{B}_{kLaB}|_r = B_{kLcD}|_r \left[ \left( \sum_{r=2}^{n} c_r B_{iJmN}|_r B^{-1}_{mNaB}|_{1r} \right) B_{cDiJ}|_{1r} + c_1 B_{cDaB}|_{1r} \right]^{-1},$$

$$r = 2 - n. \tag{34 b}$$

For the matrix we obtain from equations (28 *d*) and (32) that

$$\bar{A}_{JiAb}|_1 = \left( \sum_{r=2}^{n} c_r A_{JiMn}|_r A^{-1}_{MnAb}|_{1r} + c_1 I_{JiAb} \right)^{-1}, \quad r = 1 \tag{34 c}$$

$$\bar{B}_{kLaB}|_1 = \left( \sum_{r=2}^{n} c_r B_{iJmN}|_r B^{-1}_{mNaB}|_{1r} + c_1 I_{iJaB} \right)^{-1}, \quad r = 1. \tag{34 d}$$

Again, since the derivation from equations (28) to equations (34) is rigorous, equations (34) are exact solutions valid for statistically homogeneous multiphase composites with arbitrary microgeometry. The expressions are simplified for composites with aligned reinforcements of identical shapes, where the Eshelby tensors for all reinforcements are identical and

$$A_{JiAb}|_1 = A_{JiAb}|_{1r} = [I_{JiAb} + S^{Y}_{JiKl} Q^{0}_{KlmN} (P_{mNAb}|_1 - P^{0}_{mNAb})]^{-1}, \quad r = 2 - n, \tag{35 a}$$

$$B_{iJmN}|_1 = B_{iJmN}|_{1r} = [I_{iJmN} + S^{X}_{iJkL} P^{0}_{kLAb} (Q_{AbmN}|_1 - Q^{0}_{AbmN})]^{-1}, \quad r = 2 - n, \tag{35 b}$$

so that

$$\bar{A}_{KlAb}|_r = A_{KlCd}|_r \left( \sum_{r=1}^{n} c_r A_{CdAb}|_r \right)^{-1}, \quad r = 1 - n, \tag{36 a}$$

$$\bar{B}_{kLaB}|_r = B_{kLcD}|_r \left( \sum_{r=1}^{n} c_r B_{cDaB}|_r \right)^{-1}, \quad r = 1 - n. \tag{36 b}$$

Finally we can write

$$\bar{P}_{kLAb} = \sum_r c_r P_{kLAb}|_r A_{AbJi}|_r \left( \sum_r c_r A_{JiMn}|_r \right)^{-1}, \tag{37 a}$$

$$\bar{Q}_{KlmN} = \sum_r c_r Q_{KlbA}|_r B_{bAiJ}|_r \left( \sum_r c_r B_{iJmN}|_r \right)^{-1}. \tag{37 b}$$

In the case of composites with reinforcements of different shapes or alignments, equations (34) combined with equations (27) provide the bounds. If we ignore piezoelectricity, the elastic part of equations (37 *a*) and (37 *b*) agrees with the results of Walpole (1966a,b, 1969) and Willis (1977). The variational bounds for composites with misaligned or differently shaped reinforcements, however, have yet to be reported for elastic composites.

Since $P_{iJKl}$ and $Q_{JikL}$ are positive definite and inverses of each other, when $P^0_{iJKl} - P_{iJKl}|_r$ is positive (negative) semidefinite, $Q^0_{JikL} - Q_{JikL}|_r$ is negative (positive) semidefinite. It can be proven that these Hashin–Shtrikman-type bounds are self-consistent, which means that the upper bound on $P^*_{iJKl}$ and the lower bound on $Q^*_{JikL}$ are inverses of each other, as are the lower bound on $P^*_{iJKl}$ and the upper bound on $Q^*_{JikL}$. To show that $\bar{P}_{iJKl}$ and $\bar{Q}_{JikL}$ are indeed inverses of each other, we examine equations (30). Left multiplying equation (30 *a*) by $P_{iJKl}|_r$ and comparing the result with equation (30 *b*) yields

$$P_{iJKl}|_r\, A_{KlMn}|_r = B_{iJlK}|_r\, B^{-1}_{lKcD}|_{1r}\, P_{cDEf}|_1\, A_{EfMn}|_{1r}. \tag{38}$$

Meanwhile, left multiplying equation (30 *b*) by $Q_{JilK}|_r$ and comparing the result with equation (30 *a*) yield

$$Q_{JilK}|_r\, B_{lKnM}|_r = A_{JiKl}|_r\, A^{-1}_{KlEf}|_{1r}\, Q_{EfaB}|_1 B_{aBnM}|_{1r}. \tag{39}$$

By substituting equations (38) and (39) into equation (37), we can verify that $\bar{P}_{iJKl}$ and $\bar{Q}_{JikL}$ are indeed inverses of each other, and so the derivation of bounds for one of them also provides bounds for the other.

It is well known that, for composites with aligned reinforcements of identical shape in uncoupled elasticity, the Hashin-Shtrikman upper or lower bounds correspond to the effective moduli of the Mori–Tanaka (1973) mean-field approach, if the matrix is stiffest or most compliant phase in the composite (Weng 1992). It can be shown that it is also the case for the piezoelectric composites considered here. In such a case, the electroelastic moduli $P_{iJKl}|_1$ and $Q_{JikL}|_1$ are chosen as $P^0_{iJKl}$ and $Q^0_{JikL}$, and it is easy to verify that equations (37 *a*) and (37 *b*) are exactly the same as the expression for the effective moduli as given by the Mori–Tanaka mean-field approach (Dunn and Taya 1993b). It is noted that the Hashin–Shtrikman-type bounds for multiphase composites with reinforcements of different shapes or alignment have not been reported for pure elastic cases before, to the best knowledge of the present authors. So the current formalism can also be applied to elastic composites by ignoring piezoelectricity.

## §4. Discussion

We have derived the upper and lower bounds on the effective moduli in the sense of positive definiteness of the moduli tensors. Such bounds are physically meaningful for a subset of individual elements of the moduli tensors; most prominent are the diagonal elements which are bounded in magnitude by the corresponding elements of upper and lower bound tensors. The off-diagonal elements are not directly bounded by the corresponding elements of upper and lower bound tensors; in this case the bounds at best provide estimates of the effective moduli. At this point, one can apply the bounds to a wide range of composite microstructural geometries. To demonstrate, in this section we shall compute bounds for two-phase composites with four different microstructural geometries: continuous $PbTiO_3$- $PbZrO_3$ (PZT)-7A fibres embedded in an epoxy matrix, PZT-5A particles embedded in an epoxy matrix, a porous PZT–Pb $(Ni_{0.33}Nb_{0.67})O_3$ (PNN) ceramic and a PZT-5A/epoxy layered composite. The material properties of the constituent materials are listed in table 1 and are taken from the papers by Chan and Unsworth (1989), Bast and Wersing (1989) and Dunn and Taya (1993c). In the calculations using PZT-7A, however, the value $d_{33} = 167 \times 10^{-12}\,\mathrm{m\,V^{-1}}$ as measured by Chan and Unsworth (1989) is

Table 1. Material properties of piezoelectric ceramics and epoxy.

| Material | $C_{11}$ (GPa) | $C_{12}$ (GPa) | $C_{13}$ (GPa) | $C_{33}$ (GPa) | $C_{44}$ (GPa) | $h_{31}$ ($10^9\,V\,m^{-1}$) | $h_{33}$ ($10^9\,V\,m^{-1}$) | $h_{331}$ ($10^9\,V\,m^{-1}$) | $\beta_{11}$ ($10^9\,mF^{-1}$) | $\beta_{33}$ ($10^9\,mF^{-1}$) |
|---|---|---|---|---|---|---|---|---|---|---|
| PZT-7A | 157 | 85.4 | 73.0 | 175 | 47.2 | −1.02 | 4.58 | 2.30 | 0.246 | 0.481 |
| PZT-5A | 125 | 79.37 | 63.58 | 145 | 39.76 | −0.735 | 2.151 | 1.517 | 0.123 | 0.136 |
| PZT-5H | 154.2 | 101.2 | 84.36 | 165.7 | 42.21 | −0.50 | 1.791 | 1.130 | 0.067 | 0.077 |
| FM73 epoxy | 6.89 | 3.89 | 3.89 | 6.89 | 1.51 | 0 | 0 | 0 | 25.5 | 25.5 |
| Spurr epoxy | 8.0 | 4.4 | 4.4 | 8.0 | 1.8 | 0 | 0 | 0 | 26.9 | 26.9 |

Table 2. Outline of the procedure for calculating the bounds of piezoelectric composites.

| | |
|---|---|
| (1) | Choose the appropriate comparison material, making sure that its moduli matrix is more or less positive definite than those of constituents by checking the eigenvalues |
| (2) | Input the electroelastic moduli of the matrix, reinforcement and comparison material in positive definite form, together with the volume fraction and shape of the reinforcement |
| (3) | Transform the positive definite form of the electroelastic moduli of the comparison material to the non-positive definite form used by Dunn and Taya (1993a); use it and the shape of the reinforcement as input to evaluate the Eshelby tensors $\mathbf{S}^Z$ |
| (4) | Transform $\mathbf{S}^Z$ to $\mathbf{S}^Y$ according to equation (A 12) |
| (5) | Evaluate the concentration factor for reinforcement using equations (31) and (35) |
| (6) | Evaluate the bounds according to equations (37) |

used. Because of its importance in the calculations, it is worthwhile to discuss the choice of the comparison material. Since the piezoelectric ceramics are elastically *stiffer*, but electrically *softer* than the polymer matrix, we cannot directly choose the epoxy or the ceramic as a comparison material. We can, however, keep the elastic constants of the ceramic or polymer and increase or decrease their dielectric constants slightly to guarantee that it is the most or least positive definite of the constituent phases. The positive definiteness is verifed by computing the eigenvalues. With the comparison material so chosen, the calculation of the bounds is carried out as outlined in table 2.

### 4.1. *Fibrous composites*

Here we consider a composite consisting of continuous PZT-7A fibres embedded in an epoxy matrix. The fibres are aligned along the $x_3$ axis. This is also the unique axis for both the transversely isotropic PZT-7A fibres and the composite. Figures 2–5 show both the Voigt–Reuss- and the Hashin–Shtrikman-type bounds (or estimates)

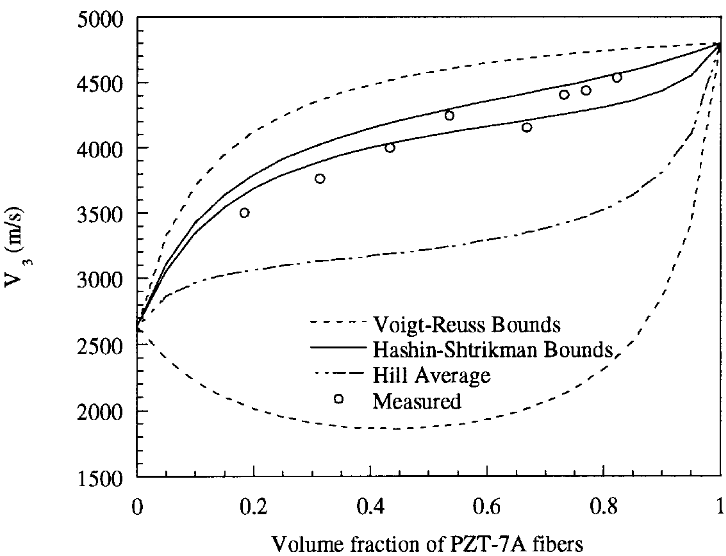


Figure 2. Bounds on the longitudinal velocity $V_3$ of the PZT-7A fibre-reinforced polymer composite versus the volume fraction of PZT-7A. The measured values are from Chan and Unsworth (1989).

for the longitudinal velocity $V_3 = (C^*_{33}/\rho)^{1/2}$, the elastic compliance $S^*_{11} + S^*_{12}$, the dielectric constant $\tau^*_{33}$ and the piezoelectric constant $d^*_{33}$ of the composite as functions of the PZT-7A fibre volume fraction. Also shown in each case is the arithmetic average of the Voigt–Reuss bounds (estimates), which in the context of elastic polycrystals and composites is known as the Hill average. Measured values of each parameter as obtained by Chan and Unsworth (1989) are also shown.

In figure 2, the density is well known to be accurately described by the rule of mixtures. Then, since the main diagonal element $C^*_{33}$ is bounded by the upper and

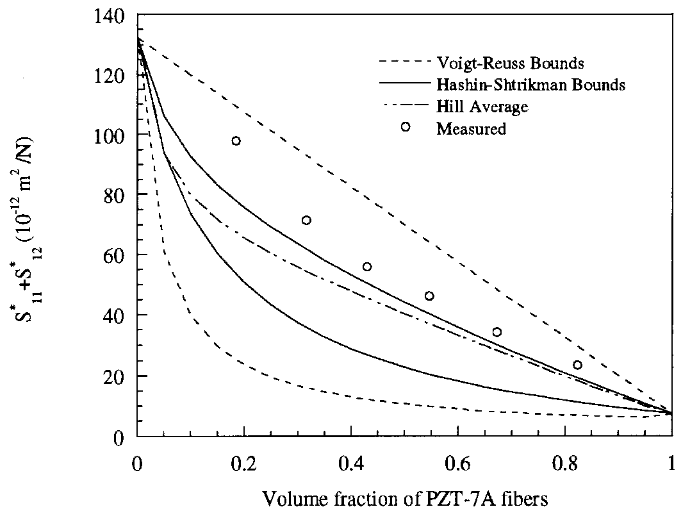


Figure 3. Bounds on $S^*_{11} + S^*_{12}$ of the PZT-7A fibre-reinforced polymer composite versus the volume fraction of PZT-7A. The measured values are from Chan and Unsworth (1989).

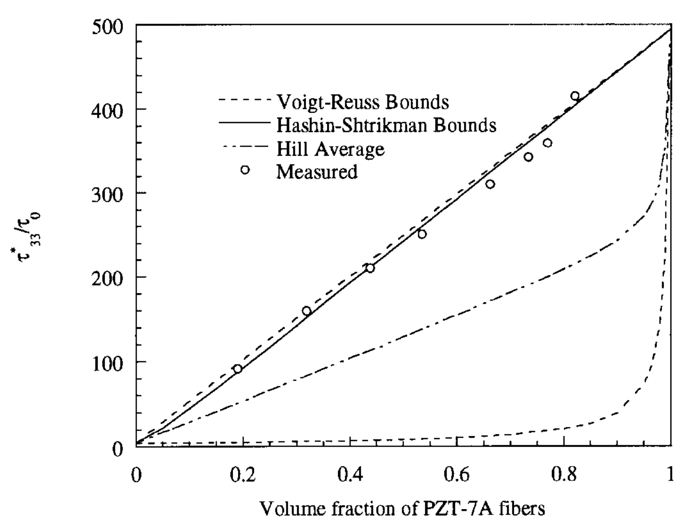


Figure 4. Bounds on $\tau^*_{33}$ of the PZT-7A fibre-reinforced polymer composite versus the volume fraction of PZT-7A. The measured values are from Chan and Unsworth (1989).

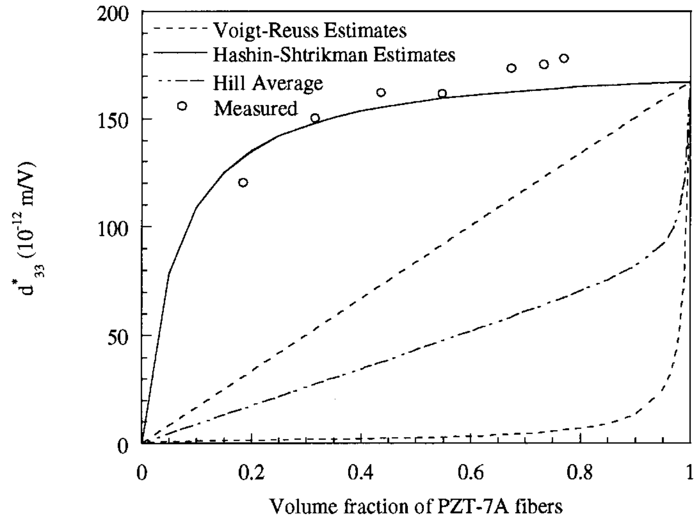


Figure 5. Estimated $d^*_{33}$ of the PZT-7A fibre-reinforced polymer composite versus the volume fraction of PZT-A. The measured values are from Chan and Unsworth (1989).

lower bounds, so is the longitudinal velocity $V_3$. It is observed that the Voigt–Reuss bounds are very wide. This is because they do not consider the shape of reinforcement, and it is extremely important. The measured data are close to the upper bound; this is because the isostrain assumption is closely approximated for the continuous fibre microstructure. The Hill average predicts the behaviour qualitatively but is not a very good quantitative predictor. Interestingly, it is far outside the Hashin–Shtrikman bounds. The Hashin–Shtrikman bounds are inside the Voigt–Reuss bounds, are quite narrow and describe the experimental data well. This is attributed to the incorporation of the reinforcement shape in their evaluation. In figures 3 and 4, $S^*_{11} + S^*_{12}$ and $\tau^*_{33}$ are bounded; the former because it is directly related to bounded quantities ($S_{11} + S_{12} = [2(S^2_{11} - S^2_{12})]/S_{66}$ for transversely isotropic symmetry, and both $S^2_{11} - S^2_{12}$ and $S_{66}$ are bounded), and the latter because it is a main diagonal element. The general observations here are similar to those of figure 2, except that in figure 3 the Hill average is inside the Hashin–Shtrikman bounds and close to the experimental data, and in figure 4 the Hashin–Shtrikman upper and lower bounds coincide with each other numerically and are in excellent agreement with measurements. The piezoelectric constant $d^*_{33}$ in figure 5 is not bounded because it is an off-diagonal element. As such, the Voigt–Reuss and Hashin–Shtrikman predictions only serve as estimates of $d^*_{33}$. Here the Voigt–Reuss estimates are quite far apart and do not agree well, either quantitatively or qualitatively, with the measurements. On the other hand, the Hashin–Shtrikman estimates agree with each other numerically and are in excellent agreement with the measurements. Interestingly, the Hill average is far from the measured data and it predicts qualitative behaviour that is grossly different from that observed.

### 4.2. *Particle-reinforced composites*

Here we consider a composite consisting of spherical PZT-5A particles embedded in an epoxy matrix. The $x_3$ axis is the unique axis for both the transversely

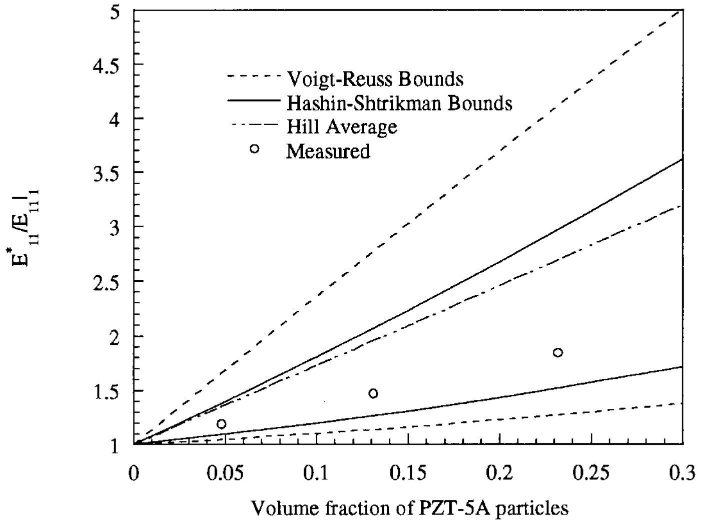


Figure 6. Bounds on $E^*_{11}$ of the PZT-5A particle-reinforced polymer composite versus the volume fraction of PZT-5A. The measured values are from Furukawa *et al.* (1976).

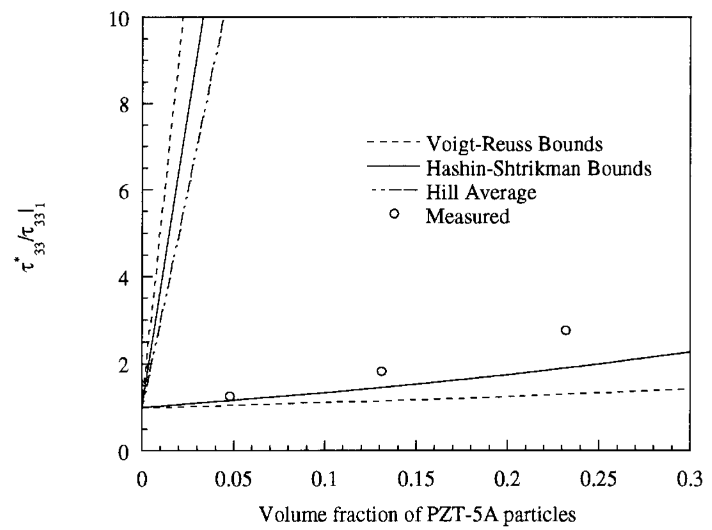


Figure 7. Bounds on $\tau^*_{33}$ of the PZT-5A particle-reinforced polymer composite versus the volume fraction of PZT-5A. The measured values are from Furukawa *et al.* (1976).

isotropic PZT-5A particles and the composite. Figures 6 and 7 show the Voigt–Reuss- and the Hashin–Shtrikman-type bounds for Young's modulus $E^*_{11}$ and the dielectric constant $\tau^*_{33}$ respectively of the composite normalized by the values for the epoxy matrix. Also shown are measured values of $E^*_{11}$ and $\tau^*_{33}$ obtained from the work of Furukawa *et al.* (1976). Again it is seen that the Hashin–Shtrikman bounds fall between and are narrower than the Voigt–Reuss bounds. The lower bounds are closer to the measurements for both $E^*_{11}$ and $\tau^*_{33}$. The bounds are much wider for $\tau^*_{33}$ than for $E^*_{11}$. This is because the difference between the $\tau_{33}$ values for the epoxy and PZT-5A is much larger than for $E_{11}$.

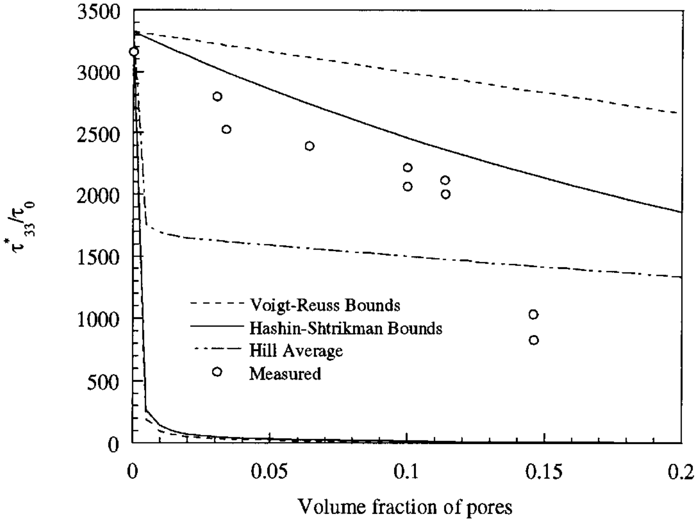


Figure 8. Bounds on $\tau^*_{33}$ of the PZT-5H ceramics with pores versus the volume fraction of pores. The measured values are from Bast and Wersing (1989).

### 4.3. *Porous ceramics*

Here we consider a porous PZT–PNN piezoelectric ceramic. Specifically, this material is a sintered PZT–PNN ceramic (transversely isotropic with the unique axis along $x_3$) with two-dimensional cylindrical voids along the $x_1$ axis. The shape of the voids is characterized by the aspect ratio $a_2/a_3$, which was measured to be 2.1 by Bast and Wersing (1989). Figure 8 shows the bounds on the dielectric constant $\tau^*_{33}$ of the porous ceramic normalized by $\tau_0$ of free space. In the calculations, the electroelastic moduli of PZT-5H were used because they are known completely (those for PZT–PNN are not) and they agree well with the known values of PZT–PNN. The elastic moduli of the pores are assumed to be zero, while the dielectric constant of the pores is taken to be the free-space dielectric constant $\tau_0 = 8.85 \times 10^{-12}\,\mathrm{C^2\,N^{-1}\,m^{-2}}$. The Hashin–Shtrikman bounds again lie inside and are much narrower than the Voigt–Reuss bounds. The Hashin–Shtrikman upper bound agrees reasonably well with the measurements at volume fractions less than about 10% but is far above the measured values at a volume fraction of about 15%. Note that the non-zero Hashin–Shtrikman lower bound is due to the non-zero dielectric constant of the pore; if it were taken to vanish, the lower bound would be zero, independent of volume fraction.

### 4.4. *Layered composites*

Finally we consider a layered composite consisting of PZT-5A ceramics and FM73 epoxy. We fabricated the composite using Colorado State University's facilities. The materials are layered along $x_3$ axis, which is the unique axis for both the transversely isotropic PZT-5A and the composite. Young's modulus for the composite was measured by Ledbetter and Kim at the National Institute of Standards and Technology, Boulder, Colorado, using a three-component oscillator. Figure 9 shows the bounds on Young's modulus $E^*_{11}$ for the layered composite. Also shown are

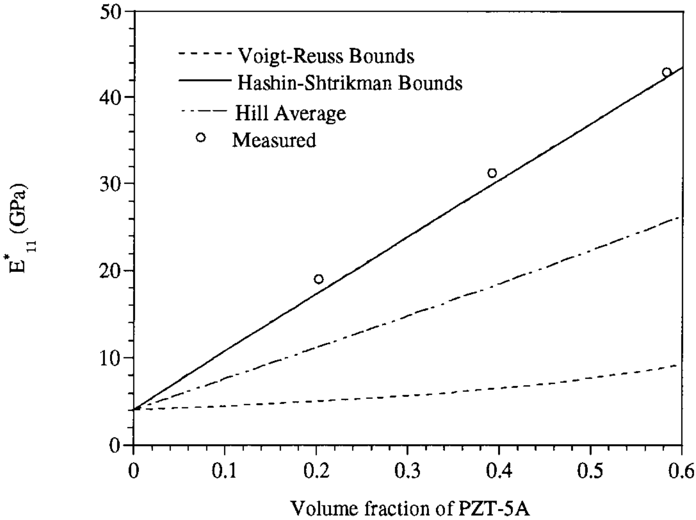


Figure 9. Bounds on $E^*_{11}$ of PZT-5A-reinforced FM73 epoxy laminate versus the volume fraction of PZT-5A.

values of $E^*_{11}$ measured by Ledbetter and Kim. In figure 9 the Hashin–Shtrikman upper and lower bounds coincide with each other numerically and are in good agreement with measurements. The reason that the measured $E^*_{11}$ is above the upper bound is that probably the elastic constants of the epoxy are slightly incorrect. The Voigt–Reuss bounds are much wider than the Hashin–Shtrikman bounds, and the Hill average does not agree with measurements well.

## § 5. Summary and conclusions

We present a method to determine the bounds of the electroelastic moduli of heterogeneous piezoelectric solids using the Hashin–Shtrikman variational principles, which is valid for statistically homogeneous multiphase composite with arbitrary microgeometry and anisotropy. Narrower bounds than the Voigt–Reuss bounds are achieved by taking into account the reinforcement shape in addition to its volume fraction. The generalized Hashin–Shtrikman bounds were shown to be self-consistent, and to agree with the Mori-Tanaka model for composites with aligned reinforcements of identical shapes if the matrix is the most positive or negative definite of all the phases. An algorithm was given for the computation of the bounds that makes use of the expressions for the electroelastic Eshelby tensors that exist in the literature. Numerical results were presented and compared with measurements for four composites with different microstructural geometries. The Hashin–Shtrikman bounds are always narrower than the Voigt–Reuss bounds and always serve as better estimates of the effective electroelastic moduli. The Hill average of the Voigt–Reuss bounds does not always agree well with measurements. Furthermore, it can predict behaviour that differs substantially from observation not only quantitatively but also qualitatively. For the cylindrical-fibre-reinforced composite and layered composite, the Hashin–Shtrikman bounds are very narrow and agree with the experimental data very well. For composites with particle inclusions, the Hashin–

Shtrikman bounds are wider and farther from measurements, suggesting that more microstructural information is required to obtain narrower bounds.

## APPENDIX A

### Electroelastic Eshelby tensors for ellipsoidal inclusions

In § 3 we obtained bounds for the effective electroelastic moduli of heterogeneous piezoelectric solids in terms of the concentration factors; in order to evaluate the bounds, we must evaluate the concentration factors. As we showed, a key part of the evaluation of the concentration factors is the evaluation of the Eshelby tensors for ellipsoidal inclusions. To this end, we take advantage of the results of Dunn and Taya (1993a) and Dunn and Wienecke (1997). The former work provides the Eshelby tensors for general material symmetry and inclusion shapes in terms of a surface integral over the unit sphere which can be easily evaluated numerically. They also obtained closed-form expressions for an elliptic cylindrical inclusion and a penny-shaped inclusion in a transversely isotropic solid. The latter work provides explicit closed-form expressions for the Eshelby tensors for spheroidal inclusions in a transversely isotropic solid. In both of these studies, a different form of the linear electroelastic constitutive equations was used. Specifically, the strain and electric field were chosen as independent variables so that the relevant eigenfields were

$$\mathrm{Z}_{\mathrm{Mn}}^{\mathrm{T}} = \begin{cases} \varepsilon_{\mathrm{mn}}^{\mathrm{T}} & \mathrm{M} = 1,2,3, \\ -\mathrm{E}_{\mathrm{n}}^{\mathrm{T}}, & \mathrm{M} = 4. \end{cases} \tag{A 1}$$

As a result, the Eshelby tensors were defined as

$$\mathrm{Z}_{\mathrm{Mn}} = \mathrm{S}_{\mathrm{MnAb}}^{\mathrm{Z}} \mathrm{Z}_{\mathrm{Ab}}^{\mathrm{T}}. \tag{A 2}$$

Here we use the superscript $Z$ to denote that the Eshelby tensors are associated with the $\mathrm{Z}_{\mathrm{Mn}}$ of equation (A 1). The superscript $Z$ was not used by Dunn and Taya and by Dunn and Wienecke. In order to take advantage of their results, first we connect $\mathrm{Y}_{\mathrm{Ji}}^{\mathrm{T}}$ of this study to their $\mathrm{Z}_{\mathrm{Mn}}^{\mathrm{T}}$. For this purpose, it is more convenient to carry out the calculations using the matrix notation described by Dunn and Taya (1993b). To this end, we rewrite equation (15) in matrix form as

$$\begin{bmatrix} \boldsymbol{\varepsilon} \\ \mathbf{D} \end{bmatrix} = \begin{bmatrix} \mathbf{S} & \mathbf{d} \\ \mathbf{d}^{\mathrm{t}} & \boldsymbol{\tau} \end{bmatrix} \left( \begin{bmatrix} \boldsymbol{\sigma} \\ \mathbf{E} \end{bmatrix} - \begin{bmatrix} \boldsymbol{\sigma}^* \\ \mathbf{E}^* \end{bmatrix} \right). \tag{A 3}$$

or in expanded form:

$$\boldsymbol{\varepsilon} = \mathbf{S}(\boldsymbol{\sigma} - \boldsymbol{\sigma}^*) + \mathbf{d}(\mathbf{E} - \mathbf{E}^*) \tag{A 4 a}$$

$$\mathbf{D} = \mathbf{d}^{\mathrm{t}}(\boldsymbol{\sigma} - \boldsymbol{\sigma}^*) + \boldsymbol{\tau}(\mathbf{E} - \mathbf{E}^*). \tag{A 4 b}$$

Caution should be taken to avoid confusion between the Eshelby tensors and the elastic compliance $\mathbf{S}$. As we just mentioned, the Eshelby tensor $\mathbf{S}^{\mathrm{Z}}$ ($\mathrm{S}_{\mathrm{jiMn}}^{\mathrm{Z}}$) is defined for the inclusion problem described by

$$\boldsymbol{\sigma} = \mathbf{C}(\boldsymbol{\varepsilon} - \boldsymbol{\varepsilon}^{\mathrm{T}}) + \mathbf{e}(-\mathbf{E} + \mathbf{E}^{\mathrm{T}}), \tag{A 5 a}$$

$$\mathbf{D} = \mathbf{e}^{\mathrm{t}}(\boldsymbol{\varepsilon} - \boldsymbol{\varepsilon}^{\mathrm{T}}) + \boldsymbol{\kappa}(-\mathbf{E} + \mathbf{E}^{\mathrm{T}}). \tag{A 5 b}$$

Because $\mathrm{Y}^{\mathrm{T}}_{\mathrm{Ji}}$ and $\mathrm{Z}^{\mathrm{T}}_{\mathrm{Mn}}$ represent transformation quantities in the same electrostatic inclusion problem, but using different notation, the field variables in equations (A 4) and (A 5) are identical. Equating the right-hand side of equations (A 4 *b*) and (A 5 *b*) yields

$$\mathsf{E}^{\mathrm{T}} = \tau^{-1}\mathbf{d}^{\mathrm{t}}\sigma^* + \mathsf{E}^*. \tag{A 6}$$

Similarly, equations (A 4 *a*) and (A 5 *a*) yield

$$\mathbf{e}\mathsf{E}^{\mathrm{T}} - \mathbf{C}\varepsilon^{\mathrm{T}} = \sigma^* + \mathbf{e}\mathsf{E}^*. \tag{A 7}$$

Substituting equation (A 6) into equation (A 7) yields

$$\varepsilon^{\mathrm{T}} = \mathbf{S}(\mathbf{e}\tau^{-1}\mathbf{d}^{\mathrm{t}} - \mathbf{I})\sigma^*. \tag{A 8}$$

Combining equations (A 6) and (A 8) yields

$$\begin{bmatrix} \varepsilon^{\mathrm{T}} \\ -\mathsf{E}^{\mathrm{T}} \end{bmatrix} = \begin{bmatrix} \mathbf{S}(\mathbf{e}\tau^{-1}\mathbf{d}^{\mathrm{t}} - \mathbf{I}) & \mathbf{0} \\ -\tau^{-1}\mathbf{d}^{\mathrm{t}} & -\mathbf{i} \end{bmatrix} \begin{bmatrix} \sigma^* \\ \mathsf{E}^* \end{bmatrix}. \tag{A 9}$$

Alternatively, this can be written as

$$\mathsf{Z}^{\mathrm{T}} = \begin{bmatrix} \mathbf{S}(\mathbf{e}\tau^{-1}\mathbf{d}^{\mathrm{t}} - \mathbf{I}) & \mathbf{0} \\ -\tau^{-1}\mathbf{d}^{\mathrm{t}} & -\mathbf{i} \end{bmatrix} \mathsf{Y}^{\mathrm{T}}. \tag{A 10}$$

Starting from consitutive equations (A 5) and applying the definition of the Eshelby tensor) $\mathbf{S}^{\mathrm{Z}}$, we have

$$\begin{aligned} \mathsf{Y} &= \begin{bmatrix} \sigma \\ \mathsf{E} \end{bmatrix} \\ &= \begin{bmatrix} \mathbf{C} & \mathbf{e} \\ \mathbf{0} & -\mathbf{i} \end{bmatrix} \begin{bmatrix} \varepsilon \\ -\mathsf{E} \end{bmatrix} - \begin{bmatrix} \mathbf{C} & \mathbf{e} \\ \mathbf{0} & \mathbf{0} \end{bmatrix} \begin{bmatrix} \varepsilon^{\mathrm{T}} \\ -\mathsf{E}^{\mathrm{T}} \end{bmatrix} \\ &= \left( \begin{bmatrix} \mathbf{C} & \mathbf{e} \\ \mathbf{0} & -\mathbf{i} \end{bmatrix} \mathbf{S}^{\mathrm{Z}} - \begin{bmatrix} \mathbf{C} & \mathbf{e} \\ \mathbf{0} & \mathbf{0} \end{bmatrix} \right) \mathsf{Z}^{\mathrm{T}}. \end{aligned} \tag{A 11}$$

Equations (A 10) and (A 11) can be combined to yield

$$\mathbf{S}^{\mathrm{Y}} = \left( \begin{bmatrix} \mathbf{C} & \mathbf{e} \\ \mathbf{0} & -\mathbf{i} \end{bmatrix} \mathbf{S}^{\mathrm{Z}} - \begin{bmatrix} \mathbf{C} & \mathbf{e} \\ \mathbf{0} & \mathbf{0} \end{bmatrix} \right) \begin{bmatrix} \mathbf{S}(\mathbf{e}\tau^{-1}\mathbf{d}^{\mathrm{t}} - \mathbf{I}) & \mathbf{0} \\ -\tau^{-1}\mathbf{d}^{\mathrm{t}} & -\mathbf{i} \end{bmatrix}. \tag{A 12}$$

Equation (A 12) allows us to compute directly the Eshelby tensors $\mathbf{S}^{\mathrm{Y}}$ (which are used in the computation of the bounds in § 3) in terms of the already tabulated $\mathbf{S}^{\mathrm{Z}}$ of Dunn and Taya (1993a). If needed, the Eshelby tensors $\mathbf{S}^{\mathrm{X}}$ can be obtained in a similar manner.

## References


Barnett, D. M., and Lothe, J., 1975, *Phys. Stat. sol.*, **67**, 105.

Bast, U., and Wersing, W., 1989, *Ferroelectrics*, **94**, 229.

Benveniste, Y., 1993a, *J. appl. Mech.*, **60**, 265; 1993b, *ibid.*, **60**, 270; 1993c, *Proc. R. Soc.* A, **441**, 59; 1994, *J. Engng Mater. Technol.*, **116**, 260.

Benveniste, Y., and Dvorak, G. J., 1992, *J. Mech. Phys. solids*, **40**, 1295.

Bisegna, P., and Luciano, R., 1996, *J. Mech. Phys. Solids*, **44**, 583.

Cao, H., Zhang, Q. M., and Cross, L. E., 1992a, *J. appl. Phys.*, **72**, 5814; 1992b, *IEEE Trans. Ultrasonics, Ferroelectrics, Frequency Control*, **40**, 103.

Chan, H. L. W., and Unsworth, J. 1989, *IEEE Trans. Ultrasonics, Ferroelectrics, Frequency Control*, **36**, 434.
Chen, T., 1993, *J. Mech. Phys. Solids*, **41**, 1781; 1994, *Int. J. Solids Struct.*, **31**, 3099; 1996, *Composites*, B, **27**, 467.
Dunn, M. L., and Taya, M., 1993a, *Proc. R. Soc.* A, **443**, 265; 1993b, *Int. J. Solids Struct.*, **30**, 161; 1993c, *J. Am. Ceram. Soc.*, **76**, 1697.
Dunn, M. L., and Wienecke, H. A., 1997, *Int. J. Solids Struct.*, **34**, 3571.
Eshelby, J. D., 1957, *Proc. R. Soc.* A, **241**, 376; 1959, *ibid.*, **252**, 561.
Furukawa, T., Fujino, K., and Fukada, E., 1976, *Jpn J. appl. Phys.*, **15**, 2119.
Grekov, A. A., Kramarov, S. O., and Kuprienko, A. A., 1989, *Ferroelectrics*, **99**, 115.
Hashin, Z., and Shtrikman, T., 1962, *J. Mech. Phys. Solids*, **10**, 343; 1963, *ibid.*, **11**, 127.
Hill, R., 1952, *Proc. Phys. Soc.* A, **65**, 349; 1964, *J. Mech. Phys. Solids.*, **12**, 199.
Hori, M., and Nemat-Nasser, S., 1998, *Mech. Mater.* **30**, 1.
Kreher, W., and Pompe, W., 1989, *Internal Stresses in Heterogeneous Solids* (Berlin: Akademie).
Li, J. Y., and Dunn, M. L., 1999, *Int. J. Engng Sci.*, **37**, 665.
Mori, T., and Tanaka, K., 1973, *Acta metall.*, **21**, 571.
Newnham, R. E., Skinner, D. P., and Cross, L. E., 1978, *Mater. Res. Bull.*, **13**, 525.
Olson, T., and Avellaneda, M., 1992, *J. appl. Phys.*, **71**, 4455.
Reuss, A., 1929, *Z. angew. Math. Mech.*, **9**, 49.
Voigt, W., 1889, *Annln Phys.*, **38**, 573.
Walpole, L. J., 1966a, *J. Mech. Phys. Solids*, **14**, 151; 1966b, *ibid.*, **14**, 289; 1969, *ibid.*, **17**, 235–251.
Weng, G. J., 1992, *Int. J. engng Sci.*, **30**, 83.
Willis, J. R., 1977, *J. Mech. Phys. solids*, **25**, 185; 1981, *Adv. appl. Mech.*, **21**, 1.